Quantum-Mechanical Study of the Collision Dynamics of $O_2(^3\Sigma_g^-) + O_2(^3\Sigma_g^-)$ on a New ab Initio Potential Energy Surface†

Jesús Pérez-Ríos, Massimiliano Bartolomei, José Campos-Martínez, Marta I. Hernández,*,‡ and Ramón Hernández-Lamoneda§

Instituto de Física Fundamental, Consejo Superior de Investigaciones Científicas, Serrano 123, 28006 Madrid, Spain, and Centro de Investigaciones Químicas, Universidad Autónoma del Estado de Morelos, 62210 Cuernavaca, Mor. México

Received: May 29, 2009; Revised Manuscript Received: September 5, 2009

The quantum mechanical theory for the scattering of two identical rigid rotors is reviewed and applied to the collision of $O_2(^3\Sigma_g^-)$ molecules using a new accurate ab initio potential energy surface (PES) for the quintet state of the composite system. The PES is based on calculations using restricted coupled-cluster theory with singles, doubles, and perturbative triple excitations [RCCSD(T)] [Bartolomei; et al. *J. Chem. Phys.* **2008**, *128*, 214304.]. This PES is extended here for large intermolecular distances using the ab initio long-range coefficients of Hettema et al. [*J. Chem. Phys.* **1994**, *100*, 1297.]. Elastic and rotationally inelastic integral cross sections have been obtained by means of close coupling calculations in the subthermal energy range (center-of-mass velocities below 500 m/s). Results are compared with those obtained using a PES derived from molecular beam experiments [Aquilanti; et al. *J. Am. Chem. Soc.* **1999**, *121*, 10794.]. General agreement is found between both PESs, although the experimentally derived PES appears as somewhat more anisotropic at least for the studied energy range. There is, however, a significant difference in the absolute value of the elastic cross sections that is due to differences in the long-range dispersion interaction. The performance of the ab initio PES for higher velocities (relevant to experiments) is also explored by retaining just the isotropic component of the interaction. A satisfactory agreement is found for the shape of the glory pattern but shifted toward lower absolute values of the cross sections.

I. Introduction

A detailed knowledge of the interactions between oxygen molecules is of interest in several areas of research. In addition to its key presence in our upper atmosphere where collisional processes compete with radiative events involving different electronic states,[1] it is of interest in several technological applications such as the Chemical Oxygen Iodine Laser,[2,3] while presenting also intriguing features in the condensed phase.[4] In addition, there is recent interest in achieving gas cooling and trapping of oxygen molecules.[5−10]

Despite the previous comments, and albeit the hypothesis on the binding of the oxygen dimer and related topics dating back to Lewis and Pauling times,[11,12] experiments and theory on the generic O_2-O_2 dimer are relatively scarce. One of the reasons for this lies in the open shell structure of the oxygen molecule that translates to the oxygen clustering. Thus, the triplet ground state of the monomers gives rise to three different potential energy surfaces (PES) of singlet, triplet, and quintet multiplicities that might exhibit different properties. This difference, and its interplay with intramolecular spin−spin coupling, is expected to play a role in the dynamics at ultralow energies.[9,10,13]

For all theses purposes an accurate knowledge of the PES is unavoidable. However, even for a small size system as this, it represents a complicated problem for ab initio studies. The problem of computing accurately weak intermolecular forces is increased by the open-shell character of the constituents which requires the use of multi configurational wave functions. Being in the limit of current theoretical methodologies, another approach would be the fruitful interplay between theory and experiment so typical in our field. In this sense it is worth mentioning that the first reliable potential was that of Bussery and Wormer[14] (BW PES), which was constructed using ab initio and semiempirical data.[15,16] Theoretical work by Bussery-Honvault et al.[17,18] based on this PES helped in a clearer understanding of the spectroscopic experiments by Campargue et al.[19,20]

As is well-known, spectroscopy probes the potential well region; thus if one intends to describe more realistically the hard wall or asymptotic behavior in a feedback process between theory and experiment, scattering measurements are better suited to this goal. In parallel with scattering experiments, the Perugia group[21,22] has produced an experimentally derived PES (hereafter referred as the Perugia PES) that has given the most accurate comparison up to date with experiments. By measuring the total integral cross section of rotationally hot and cold molecular beams of oxygen molecules colliding with target O_2 and under such conditions that glory interference effects could be observed, they were able to fit a full dimensional rigid rotor PES including the spin dependence. This PES compares qualitatively well with the previous BW PES, but, they differ in the details of the spectroscopy[17,23−25] as well as in the collision dynamics.[22]

In the meantime, new and powerful highly correlated ab initio methodologies have emerged so that some cases are able to reach spectroscopic accuracy. It has to be said that most reliable methods can be only applied to closed-shell systems (in general) or to be more specific to those systems for which single

† Part of the "Vincenzo Aquilanti Festschrift".

* Electronic mail: marta@imaff.cfmac.csic.es.

‡ Instituto de Física Fundamental, Consejo Superior de Investigaciones Científicas.

§ Universidad Autónoma del Estado de Morelos.

10.1021/jp905045b
Published on Web 10/09/2009

reference zero-order wave functions are reasonable starting points. This is the case for the quintet state of the oxygen dimer. After some preliminary studies,[26−28] we have recently presented a full-dimensional rigid rotor PES[29] computed with the restricted coupled-cluster theory with singles, doubles, and perturbative triple excitations [RCCSD(T)]. A proposition for the computation of the singlet and triplet counterparts was also presented.[27,30] In ref 29, a detailed comparison with the BW and Perugia PESs (of topographical nature) was carried out, and results for the dimer bound states were reported.

Once the complicated task of computing a good PES and a reliable fitting to a standard formulas has been achieved, the next goal consists in studying the collision dynamics, which is the purpose of the present work. In the energy domain, the most accurate dynamical procedure is solving the so-called close-coupled equations. The presence of many coupled rotational states makes the case a challenging one and only very recently for the lighter diatom−diatom collision (i.e., H_2[31]), cross sections for the very first vibrational states have been obtained. In this work we report the first accurate close coupling calculations on the $O_2 + O_2$ rotational collision dynamics, using a very recent quintet PES.[29] The PES is extended here by an adequate long-range behavior using ab initio dispersion coefficients.[32] The dynamical treatment involves the collision between two linear rigid rotors; i.e., the high frequency vibrational modes of the oxygen molecules are not taken into account in the model. In addition, the fine structure of oxygen[33] is neglected within the present treatment, although we are aware that its effects are very important in collisions at kinetic energies lower than those studied here.[9,10] The study is restricted to subthermal energies (total energies less than 175 cm^{-1}), given the rather heavy masses involved. A detailed comparison with the Perugia PES (successful in reproducing experiments performed at higher energies) is made in searching for possible improvements needed in the theoretical model.

The paper is organized as follows. Section II deals with the theory of vibrationless diatom−diatom collisions in the cases of both distinguishable and indistinguishable monomers. Details regarding application to O_2-O_2 are given in section III, and the results are reported and discussed in section IV. Finally conclusions are written in section V.

II. Theory

We first give a summary of the theory for the scattering of two closed-shell linear rigid rotors treated as distinguishable.[34,35] A discussion on the modifications in the theory for indistinguishable partners is followed.

Distinguishable Monomers. Using diatom−diatom Jacobi vectors $\mathbf{R}$, $\mathbf{r}_1$, and $\mathbf{r}_2$ in a space-fixed (SF) frame, the Hamiltonian for the interaction of two rigid rotors is written as (in atomic units),

$$H = -\frac{1}{2\mu R}\frac{\partial^2}{\partial R^2}R + \frac{\hat{l}^2}{2\mu R^2} + B(\hat{j}_1^{\,2} + \hat{j}_2^{\,2}) + V \quad (1)$$

where B is the rotational constant, μ is the reduced mass, V is the intermolecular PES, and $\hat{l}$, $\hat{j}_1$, and $\hat{j}_2$ are angular momentum operators associated with $\mathbf{R}$, $\mathbf{r}_1$, and $\mathbf{r}_2$, respectively. As the total angular momentum $\mathbf{J} = \hat{l} + \hat{j}_1 + \hat{j}_2$ commutes with H, solutions of the time-independent Schrödinger equation are written with well-defined J and J_z values and expanded as

$$\Psi_\gamma^{JM}(\mathbf{R},\hat{\mathbf{r}}_1,\hat{\mathbf{r}}_2) = \sum_{\gamma'}\frac{g_{\gamma'\gamma}^{JM}(R)}{R}I_{\gamma'}^{JM}(\hat{\mathbf{R}},\hat{\mathbf{r}}_1,\hat{\mathbf{r}}_2) \quad (2)$$

where $\gamma \equiv (j_1, j_2, j_{12}, l)$ indicates the incoming channel and $I_{\gamma'}^{JM}$ are angular functions (see eq 7 of ref 35). Substitution of eq 2 into the Schrödinger equation and integration over the angular variables lead to the well-known set of coupled differential equations for the radial coefficients $g_{\gamma'\gamma}^{JM}$.[35] After solving the close-coupled equations that lead to the Transition matrix $T_{\gamma'\gamma}^{JM}$, it only rests to connect this matrix with the scattering amplitude. The asymptotic wave function for a "physical" incoming state $\alpha \equiv \{j_1 m_1 j_2 m_2\}$ is

$$\Psi_\alpha(R\to\infty) \;\to\; \exp[i\mathbf{k}_{j_1j_2}\cdot\mathbf{R}]Y_{j_1m_1}(\hat{\mathbf{r}}_1)\,Y_{j_2m_2}(\hat{\mathbf{r}}_2) + \sum_{\alpha'}f_{\alpha'\alpha}(\hat{\mathbf{R}})\frac{\exp[ik_{j'_1j'_2}R]}{R}Y_{j'_1m'_1}(\hat{\mathbf{r}}_1)\,Y_{j'_2m'_2}(\hat{\mathbf{r}}_2) \quad (3)$$

where Y_{jm} are spherical harmonics and $k_{j_1j_2}^{\,2} = 2\mu[E - \varepsilon_{j_1} - \varepsilon_{j_2}]$, with $\varepsilon_j = Bj(j+1)$. If Ψ_α is written as a linear combination of Ψ_γ^{JM}

$$\Psi_{j_1m_1j_2m_2} = \sum_{JMj_{12}l}A_{m_1m_2}^{JMj_{12}l}\Psi_{j_1j_2j_{12}l}^{JM} \quad (4)$$

then the expansion coefficients $A_{m_1m_2}^{JMj_{12}l}$ are known by matching the incoming parts of Ψ_α and Ψ_γ^{JM} and, by comparing the scattered parts, the scattering amplitude $f_{\alpha'\alpha}(\hat{\mathbf{R}})$ and related cross sections are obtained. After summing over final m_1' and m_2' projections and averaging them over initial m_1m_2 ones, the integral cross section for a transition $j_1j_2 \to j_1'j_2'$ is given by[34,35]

$$\sigma_{j'_1j'_2j_1j_2}^{d}(k_{j_1j_2}^{\,2}) = \frac{4\pi}{k_{j_1j_2}^{\,2}\,g_{j_1}g_{j_2}}\sum_{Jj_{12}j'_{12}ll'}g_J|T_{\gamma'\gamma}^{JM}|^2 \quad (5)$$

where $g_j = 2j + 1$ and the superscript "d" indicates a cross section for distinguishable monomers.

Indistinguishable Monomers. If the colliding rotors are identical, the Hamiltonian commutes with the exchange operator, P_{12}, which changes ($\mathbf{R}$, $\mathbf{r}_1$, $\mathbf{r}_2$) to ($-\mathbf{R}$, $\mathbf{r}_2$, $\mathbf{r}_1$). Assuming that the nuclear spin of the molecules is unchanged and that the electronic state is symmetric, the observed cross section is given by[36]

$$\sigma = W^s\sigma^+ + W^a\sigma^- \quad (6)$$

where $\sigma^\pm$ are cross sections corresponding to even or odd scattering wave functions, and $W^{s,a}$ are nuclear statistical weights.

It must be pointed out that there is not complete agreement in the literature regarding the "correction" factors that must come in the symmetry adapted cross sections when $j_1 = j_2$ and/or $j_1' = j_2'$.[34,36−41] In particular, Huo and Green[41] rederived the very much cited Takayanagi's theory[34] and obtained formally different cross sections. For this reason, we have re-examined the theory and outline here our conclusions. According to Gioumousis and Curtiss,[42] the normalized incoming state with symmetry $\xi = \pm 1$ is

$$|\mathbf{k}_{j_1j_2}\alpha\xi\rangle = \frac{1}{\sqrt{2}}\{\exp[i\mathbf{k}_{j_1j_2}\cdot\mathbf{R}]Y_{j_1m_1}(\hat{\mathbf{r}}_1)\,Y_{j_2m_2}(\hat{\mathbf{r}}_2) + \xi\exp[-i\mathbf{k}_{j_1j_2}\cdot\mathbf{R}]Y_{j_2m_2}(\hat{\mathbf{r}}_1)\,Y_{j_1m_1}(\hat{\mathbf{r}}_2)\} \quad (7)$$

It is worth noting that $\{|\mathbf{k}_{j_1j_2}\alpha\xi\rangle\}$ is a complete orthonormal set, with the restriction that vectors $\mathbf{k}_{j_1j_2}$ just cover half a sphere. However, there are not restrictions for the allowed values of $\{j_1m_1j_2m_2\}$. Indeed, defining $\bar{\alpha} = j_2m_2j_1m_1$, it can be seen from eq 7 that $|\mathbf{k}_{j_1j_2}\alpha\xi\rangle$ and $|\mathbf{k}_{j_1j_2}\bar{\alpha}\xi\rangle$ *are* different states, but that $|\mathbf{k}_{j_1j_2}\alpha\xi\rangle$ and $|-\mathbf{k}_{j_1j_2}\bar{\alpha}\xi\rangle$ refer to the *same* state. It must be pointed out that in the incoming state of ref 41 an "ordered set" $\{j_1m_1j_2m_2\}$ was involved and a different normalization factor was given.

The outgoing wave is built using the same type of linear combination as for the incoming one.[42,43] After some rearrangements, it is written as[34]

$$\Psi_\alpha^{\xi\text{out}}(R\rightarrow\infty) \rightarrow \sum_{\alpha'} f^\xi_{\alpha'\alpha}(\hat{\mathbf{R}})\frac{\exp[ik_{j'_1j'_2}R]}{\sqrt{2R}}Y_{j'_1m'_1}(\hat{\mathbf{r}}_1)\,Y_{j'_2m'_2}(\hat{\mathbf{r}}_2) \quad (8)$$

where the scattering amplitude $f^\xi_{\bar{\alpha}'\alpha}$ relates to those of the distinguishable case as

$$f^\xi_{\alpha'\alpha}(\hat{\mathbf{R}}) = f_{\alpha'\alpha}(\hat{\mathbf{R}}) + \xi f_{\bar{\alpha}'\alpha}(\hat{\mathbf{R}}) \quad (9)$$

Although eq 9 allows one to obtain symmetrized cross sections from the calculation of distinguishable ones, it is computationally more convenient to adapt the wave functions of eq 2 to the symmetry. The modification only applies to the angular part:[35]

$$I^{JM\xi}_\gamma = \frac{I^{JM}_\gamma + \xi(-1)^{j_1+j_2-j_{12}+l}I^{JM}_{\bar{\gamma}}}{[2(1+\xi(-1)^{-j_{12}+l}\delta_{j_1j_2})]^{1/2}} \quad (10)$$

where $\bar{\gamma} = (j_2j_1j_{12}l)$. It must be pointed out[34] that this basis does require choosing a well ordered set ($j_1 \geq j_2$, for example). Note also that when $j_1 = j_2$, then j_{12}'s and l's such that $\xi(-1)^{-j_{12}+l} = -1$ must be excluded from the expansion (note the denominator in eq 10). Symmetry adapted T^ξ matrices are computed by solving the close-coupled equations. They are related to the unsymmetrized ones by

$$T^{JM\xi}_{\gamma'\gamma} = \frac{T^{JM}_{\gamma'\gamma} + \xi(-1)^{j'_1+j'_2-j'_{12}+l'}T^{JM}_{\bar{\gamma}'\gamma}}{[(1+\xi(-1)^{-j'_{12}+l'}\delta_{j'_1j'_2})(1+\xi(-1)^{-j_{12}+l}\delta_{j_1j_2})]^{1/2}} \quad (11)$$

Symmetrized cross sections can be obtained in a way analogous to the distinguishable ones or, alternatively, by using eqs 9 and 11 and are given as

$$\sigma^\xi_{j'_1j'_2j_1j_2}(k_{j_1j_2}{}^2) = \frac{4\pi(1+\delta_{j_1j_2})(1+\delta_{j'_1j'_2})}{k_{j_1j_2}{}^2 g_{j_1}g_{j_2}}\sum_{J j_{12}j'_{12}ll'}{}' g_J|T^{JM\xi}_{\gamma'\gamma}|^2 \quad (12)$$

where the prime in the summation symbol indicates that a restricted set $\{\gamma\}$ is used. Equation 12 agrees with the expression obtained by Takayanagi[34] and is the one used in the MOLSCAT code.[44] We believe that Huo and Green's[41] formula, in which the factors $(1+\delta_{j_1j_2})(1+\delta_{j'_1j'_2})$ are absent, is formally incorrect because of inconsistencies in their definition of the asymptotical wave function.

Distinguishable vs Indistinguishable Cross Sections. Comparison between distinguishable and indistinguishable cross sections provides insight into the effects of indistinguishability and, in addition, can be of help in the elucidation of the degeneracy or correction factors that should eventually be included. For the differential cross sections one immediately obtains from eq 9 that

$$\frac{d\sigma^\xi_{\alpha',\alpha}}{d\Omega}(k_{j_1j_2}) = \frac{k_{\gamma'}}{k_\gamma}\{|f_{\alpha'\alpha}(\hat{\mathbf{R}})|^2 + |f_{\bar{\alpha}'\alpha}(-\hat{\mathbf{R}})|^2 + 2\xi\text{Re}[f^*_{\alpha'a}(\hat{\mathbf{R}})f_{\bar{\alpha}'\alpha}(-\hat{\mathbf{R}})]\} \quad (13)$$

A distinction between two types of effects should be made. The first one can be denoted as purely classical: There are two processes (indistinguishable for the detection apparatus) in which a particle is detected with j'_1 in the $\hat{\mathbf{R}}$ direction but in one case the particle is projectile and in the other one it is target. The second effect is quantum-mechanical: it consists in the interference between the amplitudes of these two paths and is given by the third term in eq 13.

An analogous relationship is obtained for the integral cross sections. By substituting eq 11 into eq 12,

$$\sigma^\xi_{j'_1j'_2j_1j_2} = \sigma^d_{j'_1j'_2j_1j_2} + \sigma^d_{j'_2j'_1j_1j_2} + \xi\sigma^{\text{int}} \quad (14)$$

where the interference term is

$$\sigma^{\text{int}} = \frac{8\pi}{k_{j_1j_2}{}^2 g_{j_1}g_{j_2}}\sum_{J j_{12}j'_{12}ll'} g_J(-1)^{j'_1+j'_2+l'-j'_{12}}\text{Re}[T^{JM*}_{\gamma'\gamma'}T^{JM}_{\bar{\gamma}'\gamma}] \quad (15)$$

Takayanagi[34] noted that the cases $j_1 = j_2$ or $j'_1 = j'_2$, where the symmetrized cross sections become (disregarding interference effects) twice the distinguishable ones, are "exceptions". For these cases, a number of different "correction factors" have been proposed.[36−40] To look for the adequate factors, we believe that it is convenient to take into account eq 14 or 13 (neglecting for this purpose the interference terms) and study which contributions (quoting Gioumousis and Curtiss[42]) "would reasonably be considered to produce identical effects in a careful classical treatment". For this analysis it is very important to bear in mind the type of experiment one wants to simulate.

For example, if one considers the outcome $j'_1 = j'_2$ in a molecular beam experiment, it is clear that if the target is completely surrounded by counters then each collision event will be counted twice,[43] in accordance with eqs 13 and 14. However, if the integral cross section is defined from the number of particles *lost* from the incident beam, then eq 14 must divided by *two*. In this work, we correct the cross sections according to this argument:

$$\sigma^{\xi,\mathrm{corr}}_{j'_1j'_2,j_1j_2} = \frac{\sigma^{\xi}_{j'_1j'_2,j_1j_2}}{1+\delta_{j'_1j'_2}} \tag{16}$$

Obviously, much care should be taken in being consistent with the experiments or other calculations. For instance, equivalent expressions to eq 16 have been obtained by Zarur and Rabitz[36] for computing cross sections, and in recent works on ultracold $O_2 + O_2$ collisions.[9,10] However, Rabitz and Lam[38] found that the cross section consistent with their master kinetic equation must be defined as per molecule, for which the correction factor is $(1+\delta_{j_1j_2}\delta_{j'_1j'_2})(1+\delta_{j_1j_2})^{-1}(1+\delta_{j'_1j'_2})^{-1}$, and this convention has been followed by some authors.[39] Finally, Huo and Green's[41] cross section is, for practical purposes, equivalent to employing a correction factor of $(1+\delta_{j_1j_2})^{-1}(1+\delta_{j'_1j'_2})^{-1}$, which has been used by other authors.[45,46]

III. Application to O_2-O_2

Symmetries. The appropriate molecular symmetry group for describing $O_2 + O_2$ nonreactive collisions is G_{16},[17,24,47] which involves the operations of spatial inversion, E^*, permutation of nuclei within the monomers, P_1 and P_2, and simultaneous permutation of nuclei between monomers 1 and 2, P_{12}. Present calculations have been carried out with four identical nuclei of the most abundant ^{16}O isotope, i.e., bosons of zero nuclear spin. Hence the *total* wave function (electronic, nuclear spatial and nuclear spin) must be symmetric under any of the three permutations listed. Since the nuclear spin wave functions are symmetric, the product of electronic and nuclear spatial wave functions must be always symmetric.

Regarding P_1 and P_2, as the electronic wave function of the monomers is odd under these operations, the rotational wave function of the fragments must be odd. Hence the wave function expansion of eq 2 must be built using spherical harmonics with odd j_1 and j_2.

The consequences on the dynamics of the symmetry under P_{12} have been already discussed in detail in the previous section, so here we only mention details specific to the present system. For the quintet state of O_2-O_2, the electronic wave function can be written by coupling the monomers electronic spins using Clebsch Gordan coefficients[48,49] and it can be shown that this wave function is even under this operation. Hence, and taking into account that $W^s = 1$ and $W^a = 0$ (eq 4), only even cross sections (σ^+) need to be computed.

Finally, the angular basis in eq 10 is already adapted to E^* (with a parity given by $(-1)^{J+j_1+j_2+l}$ [35]). In the MOLSCAT code, cross sections for the two parity blocks are computed separately and summed up afterward.

Quintet PES. We present some details about the ab initio PES for the quintet state (total electronic spin $S = 2$) of $O_2(^3\Sigma_g^-) + O_2(^3\Sigma_g^-)$ and, specifically, on its extrapolation to large intermolecular distances. A comparison with the Perugia PES for the same multiplicity is outlined.

The ab initio PES has been obtained within the RCCSD(T) level of theory for a large set of relative orientations and intermolecular distances, while the interatomic distance within each diatom has been fixed to its equilibrium distance, $r_e = 2.28$ bohr (rigid monomers). Details of these calculations are given in ref 29. The Perugia PES, on the other hand, has been derived[22] from observed cross sections using effusive as well as supersonic seeded beams, and from data on second virial coefficients. In both cases, the interaction potential V is given by a spherical harmonics expansion as[15]

$$V(R,\theta_1,\theta_2,\phi) = (4\pi)^{3/2}\sum_{l_a,l_b,L} f^{l_al_bL}(R)\, A_{l_al_bL}(\theta_1,\theta_2,\phi) \tag{17}$$

where θ_1 and θ_2 are the angles formed by $\mathbf{R}$ and $\mathbf{r}_1$, $\mathbf{R}$ and $\mathbf{r}_2$, respectively, and ϕ is the torsional angle, and

$$A_{l_al_bL}(\theta_1,\theta_2,\phi) = \left(\frac{2L+1}{4\pi}\right)^{1/2}\sum_m \begin{pmatrix} l_a & l_b & L \\ m & -m & 0 \end{pmatrix} \times Y_{l_am}(\theta_1,0)\, Y_{l_b-m}(\theta_2,\phi) \tag{18}$$

where $Y_{l_a,m}$ and $Y_{l_b,-m}$ are spherical harmonics which are coupled with the aid of a $3-j$ symbol, and l_a, l_b, and L are even integers (due to the symmetries discussed above).

In the case of the Perugia PES, the expansion of eq 17 has four different terms with $(l_al_bL) = (000)$, (202), (220), and (222), whereas the ab initio one involves 25 additional terms (listed in ref 29), to accurately account (within 1%) for the anisotropy of the interaction. The spherically averaged terms agree quite well particularly in the repulsive region, while some differences are found in the minimum as well as in the long-range tail.[29] Both interaction potentials also agree in the geometry and well depth of the absolute minimum, in the crossed (D_{2d}) configuration, although the equilibrium distances differ.[26] More details can be found in refs 29 and 26.

The RCCSD(T) PES has been computed for $N = 18$ intermolecular distances ranging from $R_1 = 2.51$ to $R_N = 8.47$ Å (additional calculations with respect to those of ref 29 were performed for short intermolecular distances). To carry out collision dynamics calculations, it is mandatory to extend the PES with a reliable long-range interaction. There is an impressive literature about ab initio calculations of polarizabilities as well as on multipole moments for $O_2(^3\Sigma_g^-)$, and we do not intend to review it here (see ref 50 for instance, and references therein). Quadrupole and higher order moments were taken from ref 15. For the dispersion interaction, which is more significant in this system, we have taken the $C_n^{l_al_bL}$ coefficients of Hettema et al.,[32] obtained from dynamical polarizabilities calculations using response theory at the multiconfiguration self-consistent field level, and where a rather large set of coefficients has been provided. Specifically, we have taken the $C_6^{l_al_bL}(l_a,l_b = 0,2;L = 0-4)$ coefficients from the third column of Table 6 of ref 32 and the $C_8^{l_al_bL}(l_a,l_b = 0-4;L = 0-6)$ ones from the second column of the same table. In Table 1, we compare those coefficients with the Perugia ones, for the isotropic and the first anisotropic term. It can be seen that the ab initio coefficients are much smaller than those of the experimentally derived PES. The consequences of this difference will be shown and discussed in detail in the next section. It can be noted, however, that other ab initio calculations agree with that of Hettema et al. within less than 5% (see, for instance, Table 8 of ref 51 and Table 3 of ref 52).

The matching procedure between the RCCSD(T) points in the interaction region and the long-range analytical behavior has been performed as follows. For every term (l_al_bL), an additional point $R_{N+1} = 10.05$ Å in the grid of intermolecular distances was defined and assigned the energy $-C_6^{l_al_bL}/R^6 - C_8^{l_al_bL}/R^8$. Between R_1 and R_{N+1}, the energy of the term is obtained by cubic spline interpolation. For distances larger than R_{N+1}, the analytical expression is used. For those terms with no long-range coefficients available, adequate exponential functions are used for the asymptotic behavior. The procedure worked quite

TABLE 1: Long-Range Coefficients of Hettema et al. (Table VI of Ref 32), Used in This Work, for the Isotropic and the First Anisotropic Terms of the Expansion of Eq 17 [a]

$(l_a l_b L)$		ab initio	Perugia
(0 0 0)	C_6 (eV Å^6)	35.05	53.00 ± 5.0
	C_8 (eV Å^8)	261.95	
(2 0 2)	C_6 (eV Å^6)	2.53	6.12
	C_8 (eV Å^8)	81.99	

[a] Hettema's terms $(l_a l_b L)$ have been divided by $[(2l_a + 1)(2l_b + 1)(2L + 1)]^{1/2}$ to account for the same convention in the expansion. Comparison is provided with the dispersion coefficients of the experimentally derived Perugia PES.[22]

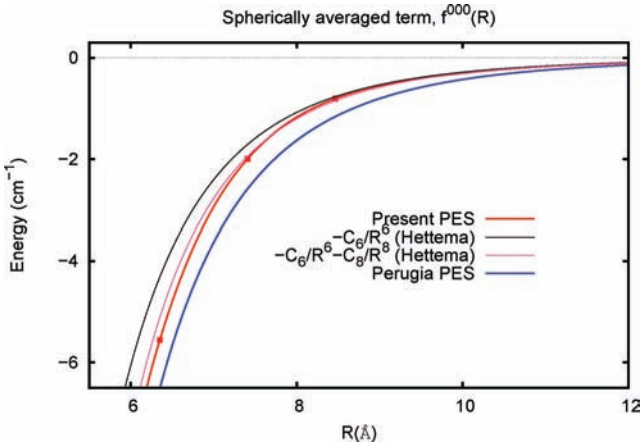

Figure 1. Comparison of intermediate and long-range behavior of the spherically averaged term for the present ab initio and Perugia quintet PESs.[22] Ab initio RCCSD(T) points are represented by filled squares. Analytical long-range behavior, used in the present PES for distances larger than 10.05 Å, is shown in the complete range for comparison: in black, only the R^{-6} term; in purple, effect of adding the R^{-8} term. See text for details.

well, indicating a good consistency between the supermolecular calculations and the calculations of the polarizabilities of the fragments.

As an example, the isotropic term is shown in Figure 1. The RCCSD(T) points are indicated by squares and the radial dependence obtained as explained above is shown by the solid line. It can be seen that a smooth behavior is achieved. Also shown in the Figure are the $-C_6/R^6$ and the complete $-C_6/R^6 - C_8/R^8$ long-range functions. It is found that, from asymptotic intermolecular distances and up to the point at 8.47 Å, the interaction is well described just by the $n = 6$ term. For shorter R's up to the next RCCSD(T) point, the induced dipole-induced quadrupole term is necessary to accurately reproduce the interaction, whereas for much shorter distances, higher order terms should be included in the expression of the dispersion interaction. Finally, it can be seen in 1 that the Perugia term, given by $-C_6/R^6$ with the coefficient of Table 1, is more attractive than the ab initio term at all intermolecular distances.

Computational Details. Integral cross sections were computed for total energies E_{tot} lower than 175 cm^{-1} using the MOLSCAT code.[44] The close-coupled equations were solved using the Alexander and Manolopoulos' hybrid log-derivative/Airy propagator.[53] The minimum intermolecular distance is fixed at 2.51 Å, and the maximum one, at 46.8 Å. At $R = 11.7$ Å, the switch between the log-derivative and the Airy propagator is done. The parameter steps, which indicates the number of integration steps per half-wavelength for the open channel of highest kinetic energy in the asymptotic region (E_k^{max}), was fixed to 5. However, given that the total energies are usually smaller than the well depth of the PES ($D_e \approx 130$ cm^{-1}), the code was modified to obtain the step size from $E_{tot} + D_e$ instead of E_k^{max}. In this way, typical step sizes for the propagation were of 0.04 Å. The maximum value of the total angular momentum J used in the calculations was chosen according to a convergence criterion of 0.5 and 0.005 Å^2 for the elastic and inelastic cross sections, respectively. About 1000 energy points were employed in the results shown in the next section. The reduced mass and rotational constants used (for ^{16}O) are 15.9994 amu and 1.438 cm^{-1}, respectively.

A total of ten rotational levels were included in the close-coupling equations, corresponding to the lowest internal energies of the fragments, i.e., $(j_1, j_2) = (1, 1)$, (1, 3), (3, 3), (1, 5), (3, 5), (1, 7), (5, 5), (3, 7), (5, 7), and (1, 9) (basis B1). This typically involves solving sets of close-coupling equations of about 300 channels for each inversion parity, total angular momentum, and energy. We have performed test calculations including four additional levels $[(j_1, j_2) = (3, 9), (7, 7), (5, 9), (1, 11)$, basis B2] to check the convergence with the rotational basis. In Table 2 we compare the cross sections for various relevant transitions. From this, we estimate that the integral cross sections reported in the next section are converged within about 5%.

TABLE 2: Convergence Test of Cross Sections (in Å^2) for Selected Transitions $(j_1, j_2) \rightarrow (j'_1, j'_2)$ at Two Different Total Enegies[a]

$(j_1, j_2) \rightarrow (j'_1, j'_2)$		$E = 80$ cm^{-1}	$E = 150$ cm^{-1}
(1, 1) → (1, 1)	B1	316.69	274.94
	B2	316.78	274.37
(1, 1) → (3, 3)	B1	17.37	13.98
	B2	17.39	13.76
(1, 1) → (3, 5)	B1	15.79	10.41
	B2	16.39	10.27
(1, 1) → all	B1	401.23	359.22
	B2	401.27	357.92
(3, 3) → (3, 3)	B1	354.97	296.21
	B2	354.19	293.51
(3, 3) → (3, 5)	B1	34.55	17.88
	B2	35.80	17.91
(3, 3) → all	B1	441.89	374.01
	B2	442.18	373.26
(3, 5) → (3, 5)	B1	433.39	317.23
	B2	441.27	314.44
(3, 5) → all	B1	514.32	389.04
	B2	522.74	387.07

[a] Total (elastic + inelastic) cross sections are indicated by $(j_1, j_2) \rightarrow$ all. Results corresponding to using 10 and 14 rotational levels in the wavefunction expansion are indicated by B1 and B2, respectively. See text for more details.

IV. Results and Discussion

Low Energy Cross Sections. In Figure 2 we report elastic and inelastic cross sections as functions of kinetic energy for the three lowest initial levels $(j_1, j_2) = (1, 1)$, (1, 3), and (3, 3) and using both the ab initio and the Perugia quintet PESs. Regarding elastic cross sections, the main noticeable difference is that the Perugia PES systematically gives larger absolute values than the ab initio one. This feature is mainly due to their different long-range behavior and is discussed in more detail in a following paragraph. For the inelastic processes, it can be seen that the ab initio and Perugia cross sections are quite similar. In general, the Perugia cross sections are somewhat larger than the ab initio ones, although the reverse becomes true for some transitions at larger kinetic energies (note also that the (1, 1) → (1, 5) ab initio cross section is larger in the

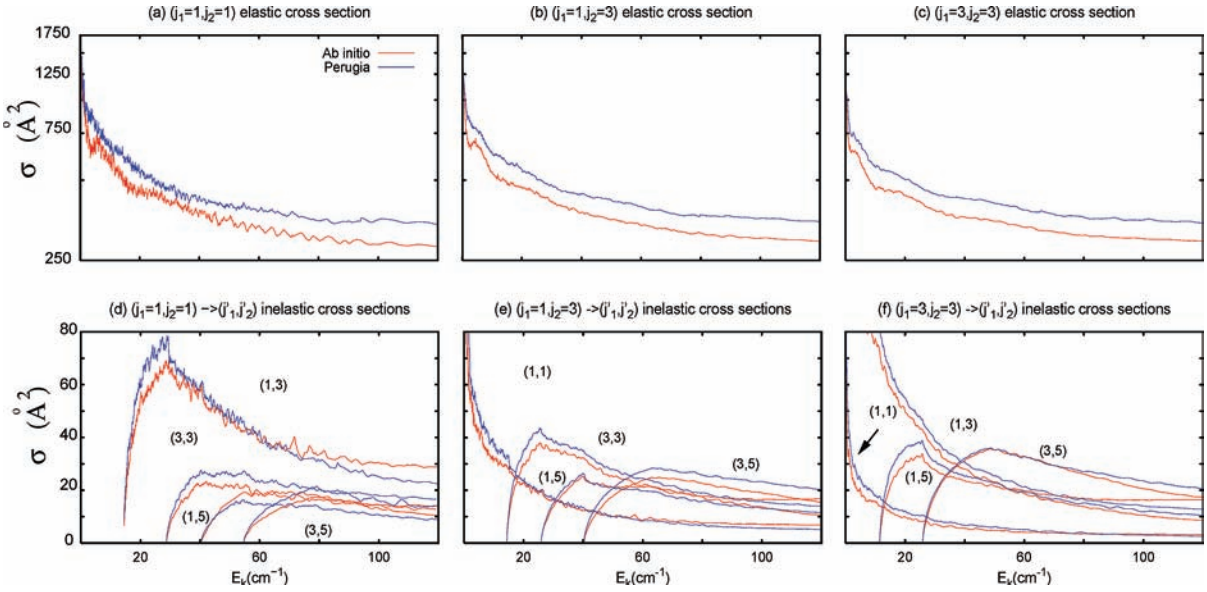

Figure 2. Elastic (upper panels, in logarithmic scale) and inelastic (lower panels) integral cross sections (in Å^2) as functions of kinetic energy (in cm^{-1}), obtained by means of close-coupling calculations. Results using the ab initio quintet PES are reported in red and those corresponding to the experimentally derived PES, in blue. Initial rotational levels $(j_1, j_2) = (1, 1)$, (1, 3), and (3, 3) correspond to the first, second, and third columns, respectively, and final levels (j'_1, j'_2) for the inelastic transitions are indicated inside the panels. See text for discussion.

whole range). Thus, it appears that the Perugia PES is "more anisotropic" at least for low energy transitions. This result has been somewhat surprising to us because in a previous work[29] it was concluded that the ab initio PES is more anisotropic. Indeed, it was found that the potential wells at the limiting geometries (rectangular, crossed, T-shaped and linear) differ much more among each other in the ab initio than in the Perugia PES. Clearly this larger anisotropy is not revealed in rotational transitions at low energies.

On the other hand, it can be seen in Figure 2 that cross sections involving the initial and/or final $(j_1, j_2) = (1, 1)$ level are much more structured than cross sections for other levels. This equally happens for the ab initio and the Perugia PES. After some analysis of the contributions to the cross section (see eq 12), we have found that, for every transition involving a pair of (j_1, j_2) and (j'_1, j'_2) levels, all the state-to-state cross sections $\gamma \rightarrow \gamma'$ are very structured (with glory interference and resonance features). However, the transitions involving the (1, 3) and (3, 3) levels appear much less structured than the (1, 1) one because they involve an average over a much larger set of $\gamma \rightarrow \gamma'$ cross sections. On passing, we note that some test calculations were performed to compare indistinguishable and distinguishable cross sections and it was found that interference effects due to indistinguishability are negligible at the kinetic energies studied.

To discuss in more detail the behavior of the elastic and total cross sections, it is useful to consider a semiclassical formula due to Landau and Lifshitz[54] and Schiff[55] for the cross section between structureless particles interacting through a long-range potential $-C_6/R^6$ (see also ref 56). It gives a constant behavior for the cross section multiplied by $v^{2/5}$, being v the center-of-mass velocity,

$$\sigma(v) \times v^{2/5} \equiv Q(C_6) = p\left(\frac{C_6}{\hbar}\right)^{2/5} \qquad (19)$$

where $p = 8.083$. In 3 we plot $\sigma(v) \times v^{2/5}$ as a function of velocity, for three cases (i) the $(j_1, j_2) = (1, 3)$ elastic cross section, (ii) the total (elastic + inelastic) cross section for the same initial state, and (iii) the quantum cross section between two structureless particles of mass μ interacting with the *isotropic* component of the PES (atom−atom model). In addition, the value within the semiclassical model, $Q(C_6)$, is displayed by a horizontal line.

We discuss first the features of Figure 3 common to the two PESs under study. The cross section for the atom−atom model shows an interference pattern with an envelope that oscillates around the value $Q(C_6)$ predicted by the semiclassical model. This behavior is due to the glory effect (note that there are also a few pronounced peaks due to orbiting resonances). For the complete close-coupling calculation, it can be seen that both elastic and total cross sections also exhibit glory structures, but considerably quenched and with displaced maxima and minima with respect to the atom−atom model. This is the expected trend since the complete calculation introduces many more state-to-state transitions within an anisotropic potential, with the result of a quenching of the interference pattern. Importantly, it is found that the *total* cross section coincides on average with $Q(C_6)$; i.e., its absolute value is given, at zero order, by the long-range behavior of the isotropic term. In addition, from the comparison with the elastic cross section, it can be seen that inelastic events contribute significantly to the total cross section.

With respect to the comparison between the ab initio and Perugia PESs, it can be observed from Figure 3 that the glory pattern in the full calculation for the Perugia PES is more quenched that in the case of the ab initio PES. This is probably due to the effect of the anisotropy of the Perugia PES in this energy range, already discussed above. However, the most important difference between both PESs is the absolute values of the cross sections, which in turn are due to the very different values of the long-range coefficients of the isotropic component (see Table 1). It is convenient to note the different origin of the long-range coefficients: the ab initio coefficients are obtained from calculations of dynamic polarizabilities,[32] while the coefficient of the Perugia PES was derived from measurements of total cross sections[22] at higher velocities than those considered here.

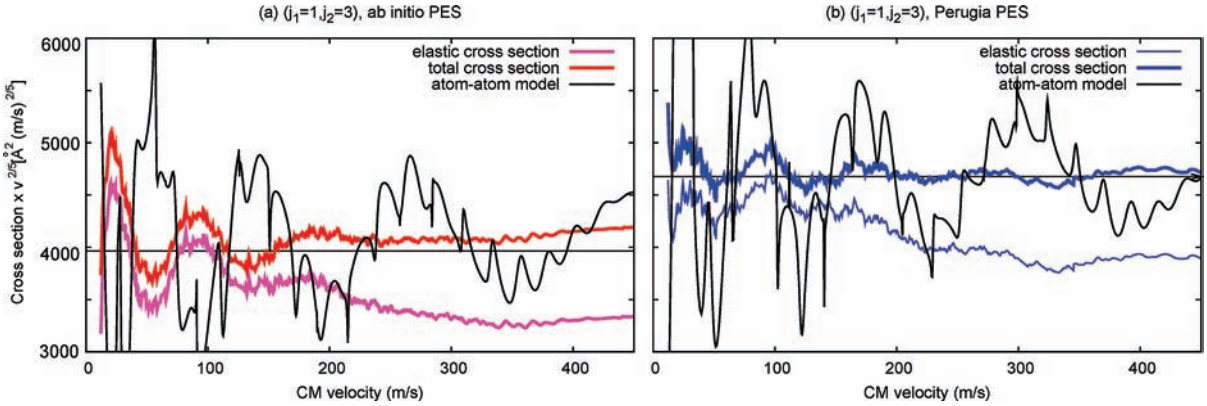

Figure 3. Elastic and total (elastic + inelastic) integral cross sections, multiplied by $v^{2/5}$ (in Å^2 (m/s)$^{2/5}$), as functions of v, the center-of-mass velocity (in m/s). In black are given the cross sections obtained by just retaining the isotropic component of the interaction (atom−atom model). In addition, the horizontal line shows the semiclassical estimation for an interaction given by $-C_6/R^6$ (see eq 19). The initial rotational levels are $(j_1, j_2) = (1,3)$ and the results corresponding to the present ab initio and Perugia quintet PESs are shown in the left and right panels, respectively.

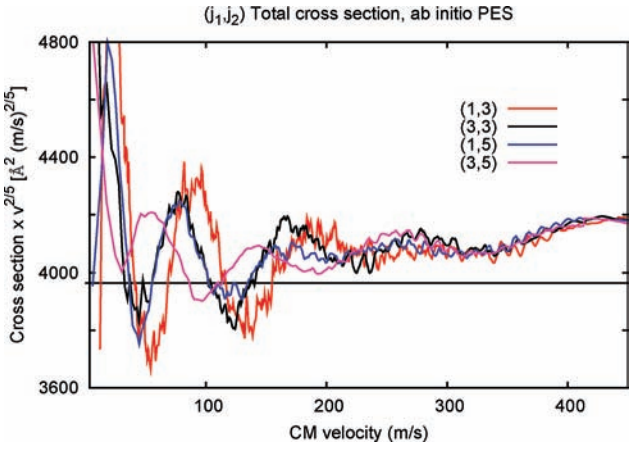

Figure 4. Effect of the selection of the initial rotational level in the total (elastic + inelastic) cross sections as functions of the center-of-mass velocity v. Also shown is the semiclassical estimation of eq 19 (horizontal line). Results shown correspond to the ab initio PES.

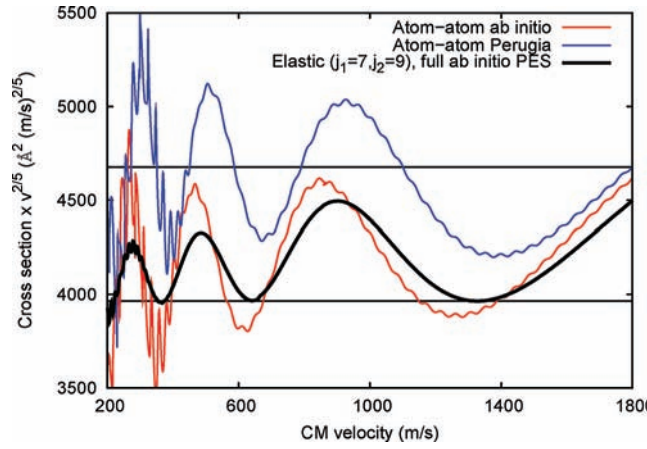

Figure 5. Cross sections (multiplied by $v^{2/5}$, in Å^2 (m/s)$^{2/5}$) as functions of the center of mass velocity v (in m/s), within the atom−atom model where just the spherically averaged term of the interaction is retained. Results corresponding to the ab initio and Perugia quintet PESs under comparison are shown in red and blue, respectively. Semiclassical estimations (eq 19) using the two PESs are also given by the constant lines. In black, it is shown the effect of including the anisotropy of the ab initio PES and transitions between magnetic levels for the initial rotational state $(j_1, j_2) = (7,9)$. See text for discussion and details of the calculations.

In Figure 4, we present a comparison of the total (elastic + inelastic) cross sections for different initial levels (j_1, j_2), using the ab initio PES. It can be seen that, while differing at low velocities, they tend to the same value at the highest velocities. It is worthwhile to comment that this result has been achieved by using the convention of eq 16 (i.e., other correction factors in the literature would give different absolute values of the cross sections at large velocities). Finally, it can be seen that the cross sections tend, for the higher velocities, toward values larger than those predicted by the long-range coefficient C_6 of the isotropic component. The origin of this behavior is discussed below.

Toward a Comparison with Experiments at Higher Energies. It would be really interesting to test the present ab initio PES against the total cross sections measured by the Perugia group[21,22] (together with those corresponding to the singlet and triplet multiplicities, in progress). However, the experiments involve quite high beam velocities (between 500 and 2000 m/s in the laboratory frame) and, in the case of effusive beams, high initial rotational states (most populated levels j_1 and j_2 between 9 and 13). In these conditions the close-coupling calculations become prohibitive due to the increasing number of channels and partial waves that should be included.

However, it is reasonably expected[57] that inelastic processes become less probable for high initial rotational levels and that the use of an atom−atom model using the spherically averaged potential will become more realistic than in the case of low energy and low rotational states collisions. Thus, we have employed in this section the atom−atom and other simple dynamical models for obtaining cross sections at higher energies. The aim is discussing in a qualitative way the performance of the ab initio PES and the ingredients that should be added to the theory to simulate in a realistic way the experiments for these challenging conditions.

In Figure 5 we present the cross sections for the atom−atom model using the two PESs under study. This calculation has been performed using the MOLSCAT code including only the $(j_1, j_2) = (0, 0)$ rotational level and just the isotropic component of the interaction. It is convenient to point out that the same results are achieved by using different rotational levels as well as a semiclassical method:[58] these calculations only bring differences in the fine structure of the cross sections and not in the main envelope, so we do not show them here for clarity. The most interesting result is the different behavior of the ab initio and Perugia PESs at intermediate velocities. While the Perugia cross section keeps, in average, a value given by $Q(C_6)$,

the ab initio one tends, on average, toward absolute values higher than that predicted by the $Q(C_6)$ estimation. Note that this trend was also found in the total cross sections of the complete close-coupling calculation (Figure 4). This behavior is due to the shape of the PESs at relevant intermolecular distances. For velocities in the range 600−900 m/s, the absolute value of the cross section is sensitive to the potential features at distances of about 6−7 Å. In this region, the Perugia PES is given exactly by $-C_6/R^6$,[22] whereas the ab initio PES needs to be described by higher order dispersion coefficients (see Figure 1). It well-known[57] that the experimentally derived C_6 coefficient must be considered as an effective term, since in the R range probed by the experiments, higher order induced multipole-induced multipole interactions play a significant role.

Center-of-mass velocities relevant for the experiments using effusive beams range between 300 and 2000 m/s. The spherically averaged quintet Perugia PES studied here, together with the corresponding singlet and triplet PESs and within the atom−atom model, provide an almost perfect agreement with the observed cross sections.[22] Within the limitations of the atom−atom model, it can be anticipated that the present ab initio PES will provide a reasonable agreement regarding the positions and amplitudes of the maxima and minima of the glory undulations, but it will fail in reproducing the average absolute value of the cross sections. Given the level of theory of the electronic structure calculations [RCCSD(T)] and the use of a large basis,[29] we do not expect that even more accurate ab initio calculations will modify the interaction energies at the relevant intermolecular distances so as to increase significantly the absolute value of the cross section. It would be worthwhile, however, to check this statement in future investigations.

On the other hand, from the complete close-coupling calculations, it has been found that the total cross sections tend, on average and as the velocity increases, to absolute values larger than those given by the $Q(C_6)$ value (Figure 4). Certainly, this is due (at least in part) to the effect of the higher order terms of the dispersion interaction, as explained above. However, it is also found that inelastic processes are quite important for a quantitative estimation of the total cross section (see Figure 3 for instance). We do not expect that for higher rotational levels the inelastic processes become negligible since, contrary to the atom−diatom case,[57] a larger density of rotational levels exists. However, it is unclear that inelastic processes will modify the average value of the *total* cross section. We think that it is interesting to study the role of the rotational transitions for higher total collision energies and this could be performed by means of less demanding treatments such as the coupled states approximation.[59]

Another effect that should play a role even in the *elastic* cross sections[60] is the anisotropy of the PES in modifying the state-to-state transitions $j_1m_1j_2m_2 \rightarrow j_1m_1'j_2m_2'$ and thus in shaping $\sigma_{j_1j_2\rightarrow j_1'j_2'}$ after averaging over m_1, m_2, m_1', m_2'. We have carried out a test close-coupling calculation restricted only to the (j_1, j_2) = (7, 9) *level* (which is expected to be populated in the experiment) but including all the magnetic sublevels and the whole anisotropy of the ab initio PES. The result is shown in Figure 5 by the black line. It can be seen that elastic (but magnetic levels changing) transitions quench the glory oscillations and modify the positions of the extrema toward larger velocities. This modification should bring a noticeable effect in the simulation of the observed cross sections. Similar test calculations in O_2−Kr also obtained a reduction of the glory amplitude but not a shift in the position of the glory extrema.[57]

Finally, it must be noted that the rotational levels of oxygen molecules in their ground electronic state $^3\Sigma_g^-$ undergo a non-negligible splitting due to second-order spin−orbit and spin−spin couplings[33] with a coupling constant of the order of the rotational constant B. Inclusion of these terms in the Hamiltonian for the O_2-O_2 interaction is essential in the study of collisions at low and ultralow[9,10] energies. Interestingly, such an intramolecular fine structure brings modifications and splittings of the singlet, triplet, and quintet intermolecular potentials.[9,10,47] It would be interesting to investigate if it will modify in a significant manner the effective long-range behavior of the intermolecular interaction. Studies in the directions mentioned above are planned for the future.

V. Summary and Conclusions

Elastic and rotationally inelastic cross sections for the collision of two vibrationless oxygen molecules have been computed using quantum scattering methodology with full dimensionality. Special care has been taken to properly include the symmetry with respect to interchange of identical particles. Two potential energy surfaces are analyzed: a recently developed ab initio potential surface of high accuracy for the quintet state and the most reliable experimentally derived potential of the Perugia group. One of the main drives for this work is that the accurate determination of the interaction potential for two oxygen molecules has remained a challenging problem for both theory and experiment and although there exists overall agreement in the main features there are still important discrepancies in the quantitative determination of the finer details. In this sense the calculation of the collision dynamics allows a detailed probing of subtle properties of the interaction potential. Furthermore, the experimental determination of the interaction potential depends on dynamical approximations for the collision process which can now be put to a test.

The predicted elastic cross sections (low initial rotational states) for both potentials show the expected kinetic energy dependence but the Perugia potential leads to larger absolute values. This can be directly related to the differences in the description of the long-range tail of the interaction, more specifically, to the more attractive terms included in the Perugia PES. On the basis of many independent and reliable estimates of the dispersion coefficients we conclude that the Perugia potential overestimates the value of the C_6 coefficient of the isotropic interaction, since at the intermolecular distances probed by the experiments, higher order induced multipole-induced multipole interactions are playing a significant role. The inelastic cross sections predicted with both potentials are very similar but again the absolute values are larger in the case of the Perugia PES. This indicates a higher anisotropy that would have been difficult to predict based on the topography of the surfaces. A test of the anisotropy of the O_2-O_2 interaction could be done by means of combined experimental-theoretical studies of the evolution of rotational populations measured by Raman spectroscopy along supersonic free jets expansions, as recently done for N_2-N_2.[45]

These findings might have implications in understanding the behavior of oxygen molecules at very low temperatures. Very recently, Tscherbul et al.[10] used the Perugia PES in quantum mechanical calculations of cold and ultracold $O_2 + O_2$ collisions in a magnetic field. They found that magnetic spin relaxation is generally very efficient and thus evaporative cooling would be very difficult to achieve. The mechanism for spin depolarization[13] involves couplings between rotational levels and hence the anisotropy of the PES plays a determinant role. The ab initio

PES, as is less anisotropic at low energies, could improve the present prospects for evaporative cooling. In addition, the different long-range interaction might change the features of the suppression of spin-changing transitions at low energies and magnetic fields. A *d*-wave centrifugal barrier in the exit channel (due to conservation of the angular momentum projection) is the cause of the suppression of the relaxation process.[9] The smaller ab initio C_6 coefficient makes the height of the *d*-wave barrier higher and this could allow evaporative cooling at somewhat higher magnetic fields than those predicted in ref 10. It would be very interesting to carry out calculations as those presented in ref 10 using the new ab initio PES. To this end, ab initio PESs for the singlet and triplet multiplicities are needed.[30] Work in this direction is underway.

Fine structure of the monomers has not been considered in the present treatment. Spin-dependent interactions, being determinant in cold collisions, could also play a role in the energy range studied here, given the extreme sensitivity of the cross sections to the long-range tail of the potential. Future investigations should include these interactions. Moreover, it would be interesting to study the collision dynamics at higher energies (using approximations such as helicity decoupling), and perform simulations of the experiments using supersonic seeded beams with control of the molecular alignment.[21,22] Efforts in these directions are in progress.

Acknowledgment. We acknowledge financial support by MEC (Spain, grant CTQ2007-62898-BQU) and by binational CSIC-CONACYT program J110.483. M.B. was supported by JAE-doc CSIC grants, and J.P.-R. by a predoctoral JAE CSIC grant. We also thank CESGA (Spain) for allocation of computing time.

References and Notes

(1) Slanger, T. G.; Copeland, R. A. *Chem. Rev.* **2003**, *103*, 4731.
(2) Antonov, I. O.; Azyazov, V. N.; Ufimtsev, N. I. *J. Chem. Phys.* **2003**, *119*, 10638.
(3) Liu, J.; Morokuma, K. *J. Chem. Phys.* **2005**, *123*, 204319.
(4) Freiman, Y. A.; Jodl, H. J. *Phys. Rep.* **2004**, *401*, 1.
(5) Friedrich, B.; deCarvalho, R.; Kim, J.; Patterson, D.; Weinstein, J. D.; Doyle, J. M. *J. Chem. Soc., Faraday Trans.* **1998**, *94*, 1783.
(6) Weinstein, J.; deCarvalho, R.; Guillet, T.; Friedrich, B.; Doyle, J. M. *Nature* **1998**, *395*, 148.
(7) Patterson, D.; Doyle, J. M. *J. Chem. Phys.* **2007**, *126*, 154307.
(8) Narevicius, E.; Libson, A.; Parthey, C. G.; Chavez, I.; Narevicius, J.; Even, U.; Raizen, M. G. *Phys. Rev. A* **2008**, *77*, 051401.
(9) Avdeenkov, A. V.; Bohn, J. L. *Phys. Rev. A* **2001**, *64*, 052703.
(10) Tscherbul, T. V.; Suleimanov Yu, V.; Aquilanti, V.; Krems, R. V. *New J. Phys.* **2009**, *11*, 055021.
(11) Lewis, G. N. *J. Am. Chem. Soc.* **1924**, *46*, 2027.
(12) Pauling L. *The nature of the chemical bond*; Cornell University Press: Ithaca, NY, 1960.
(13) Krems, R. V.; Dalgarno, A. *J. Chem. Phys.* **2004**, *120*, 2296.
(14) Bussery, B.; Wormer, P. E. S. *J. Chem. Phys.* **1993**, *99*, 1230.
(15) Wormer, P. E. S.; van der Avoird, A. *J. Chem. Phys.* **1984**, *81*, 1929.
(16) Cambi, R.; Cappelletti, D.; Liuti, G.; Pirani, F. *J. Chem. Phys.* **1991**, *95*, 1852.
(17) Bussery-Honvault, B.; Veyret, V. *Phys. Chem. Chem. Phys.* **1999**, *1*, 3387.
(18) Bussery-Honvault, B.; Veyret, V.; Umanskii, S. Ya. *Phys. Chem. Chem. Phys.* **1999**, *1*, 3395.
(19) Campargue, A.; Biennier, L.; Kachanov, A.; Jost, R.; Bussery-Honvault, B.; Veyret, V.; Churassy, S.; Bacis, R. *Chem. Phys. Lett.* **1998**, *288*, 734.
(20) Biennier, L.; Romanini, D.; Kachanov, A.; Campargue, A.; Bussery-Honvault, B.; Bacis, R. *J. Chem. Phys.* **2000**, *112*, 6309.
(21) Aquilanti, V.; Ascenzi, D.; Bartolomei, M.; Cappelletti, D.; Cavalli, S.; de Castro Vítores, M.; Pirani, F. *Phys. Rev. Lett.* **1999**, *82*, 69.
(22) Aquilanti, V.; Ascenzi, D.; Bartolomei, M.; Cappelletti, D.; Cavalli, S.; de Castro Vítores, M.; Pirani, F. *J. Am. Chem. Soc.* **1999**, *121*, 10794.
(23) Aquilanti, V.; Bartolomei, M.; Cappelletti, D.; Carmona-Novillo, E.; Pirani, F. *Phys. Chem. Chem. Phys.* **2001**, *3*, 3891.
(24) Aquilanti, V.; Carmona-Novillo, E.; Pirani, F. *Phys. Chem. Chem. Phys.* **2002**, *4*, 4970.
(25) Carmona-Novillo, E.; Pirani, F.; Aquilanti, V. *Int. J. Quantum Chem.* **2004**, *99*, 616.
(26) Hernández-Lamoneda, R.; Hernández, M. I.; Campos-Martínez, J. *Chem. Phys. Lett.* **2005**, *414*, 11.
(27) Hernández-Lamoneda, R.; Bartolomei, M.; Hernández, M. I.; Campos-Martínez, J.; Dayou, F. *J. Phys. Chem. A* **2005**, *109*, 11587.
(28) Hernández-Lamoneda, R.; Bartolomei, M.; Carmona-Novillo, E.; Hernández, M. I.; Campos-Martínez, J.; Dayou, F. In *Beyond standard quantum chemistry: Applications from gas to condensed phases*; Hernández-Lamoneda, R., Ed.; Transworld Research Network, 2007; ISBN 978-81-7895-293-2.
(29) Bartolomei, M.; Carmona-Novillo, E.; Hernández, M. I.; Campos-Martínez, J.; Hernández-Lamoneda, R. *J. Chem. Phys.* **2008**, *128*, 214304.
(30) Bartolomei, M.; Hernández, M. I.; Campos-Martínez, J.; Carmona-Novillo, E.; Hernández-Lamoneda, R. *Phys. Chem. Chem. Phys.* **2008**, *10*, 5374.
(31) Otto, F.; Gatti, F.; Meyer, H.-D. *J. Chem. Phys.* **2008**, *128*, 064305.
(32) Hettema, H.; Wormer, P. E. S.; Jorgensen, P.; Jensen, H. J. Aa.; Helgaker, T. *J. Chem. Phys.* **1994**, *100*, 1297.
(33) Mizushima M. *The Theory of Rotating Diatomic Molecules*; Wiley: New York, 1975.
(34) Takayanagi, K. *Adv. At. Mol. Phys.* **1965**, *1*, 149.
(35) Green, S. *J. Chem. Phys.* **1975**, *62*, 2271.
(36) Zarur, G.; Rabitz, H. *J. Chem. Phys.* **1974**, *60*, 2057.
(37) Takayanagi, K. *Prog. Theor. Phys. (Kyoto) Suppl.* **1963**, *25*, 1.
(38) Rabitz, H.; Lam, S.-H. *J. Chem. Phys.* **1975**, *63*, 3532.
(39) Schaefer, J.; Meyer, W. *J. Chem. Phys.* **1979**, *70*, 344.
(40) Danby, G.; Flower, D. R.; Monteiro, T. S. *Mon. Not. R. Astron. Soc.* **1987**, *226*, 739.
(41) Huo, W. M.; Green, S. *J. Chem. Phys.* **1996**, *104*, 7572.
(42) Gioumousis, G.; Curtiss, C. F. *J. Chem. Phys.* **1958**, *29*, 996.
(43) Taylor J. R. *Scattering Theory: The Quantum Theory on Nonrelativistic Collisions*; John Wiley and Sons: New York, 1972.
(44) Hutson J. M.; Green S. *molscat version 14; Collaborative Computational Project No. 6*; U.K. Science and Engineering Research Council, 1994.
(45) Fonfría, J. P.; Ramos, A.; Thibault, F.; Tejeda, G.; Fernández, J. M.; Montero, S. *J. Chem. Phys.* **2007**, *127*, 134305.
(46) Lee, T.-G.; Balakrishnan, N.; Forrey, R. C.; Stancil, P. C.; Shaw, G.; Schultz, D. R.; Ferland, G. J. *Astrophys. J.* **2008**, *689*, 1105.
(47) van der Avoird, A.; Brocks, G. *J. Chem. Phys.* **1987**, *87*, 5346.
(48) Dayou, F.; Hernández, M. I.; Campos-Martínez, J.; Hernández-Lamoneda, R. *J. Chem. Phys.* **2005**, *123*, 74311.
(49) Zarur, G. L.; Chiu, Y. *J. Chem. Phys.* **1972**, *56*, 3278.
(50) Minaev, B. *Spectrochim. Acta Part A* **2004**, *60*, 1027.
(51) Spelsberg, D.; Meyer, W. *J. Chem. Phys.* **1998**, *109*, 9802.
(52) Zuchowski, P. S. *Chem. Phys. Lett.* **2008**, *450*, 203.
(53) Manolopoulos, D. E.; Alexander, M. H. *J. Chem. Phys.* **1987**, *86*, 2044.
(54) Landau L. D.; Lifshitz E. M. *Quantum Mechanics*; Pergamon Press Ltd.: London, 1959.
(55) Schiff, L. I. *Phys. Rev.* **1956**, *103*, 443.
(56) Bernstein, R. B.; Kramer, K. H. *J. Chem. Phys.* **1963**, *38*, 2507.
(57) Aquilanti, V.; Ascenzi, D.; Cappelletti, D.; de Castro-Vítores, M.; Pirani, F. *J. Chem. Phys.* **1998**, *109*, 3898.
(58) Pirani, F.; Vecchiocattivi, F. *Mol. Phys.* **1982**, *45*, 1003.
(59) Heil, T. G.; Green, S.; Kouri, D. J. *J. Chem. Phys.* **1978**, *68*, 2562.
(60) Dagdigian, P. J.; Alexander, M. H. *J. Chem. Phys.* **2009**, *130*, 094303.

JP905045B